RESEARCH ARTICLE

Rapid Communications in Mass Spectrometry   WILEY

Matrix-assisted laser desorption/ionization-Fourier-transform ion cyclotron resonance-mass spectrometry analysis of exosomal lipids from human serum

Iqbal Jalaludin[1] [ID] | Huu-Quang Nguyen[1] [ID] | Kyoung-Soon Jang[2] |
Jaebeom Lee[1,3] | David M. Lubman[4] | Jeongkwon Kim[1,5] [ID]

[1]Department of Chemistry, Chungnam National University, Daejeon, Republic of Korea

[2]Biomedical Omics Center, Korea Basic Science Institute, Cheongju, Republic of Korea

[3]Department of Chemical Engineering and Applied Chemistry, Chungnam National University, Daejeon, Republic of Korea

[4]Department of Surgery, University of Michigan Medical Center, Ann Arbor, Michigan

[5]Graduate School of New Drug Discovery and Development, Chungnam National University, Daejeon, Republic of Korea

Correspondence
J. Kim, Graduate School of New Drug Discovery and Development, Chungnam National University, Daejeon, Republic of Korea.
Email: jkkim48105@cnu.ac.kr

Rationale: Exosomes contain biomarkers such as proteins and lipids that help in understanding normal physiology and diseases. Lipids, in particular, are infrequently studied using matrix-assisted laser desorption/ionization (MALDI) mass spectrometry (MS) for biomarker discovery. In this study, MALDI was equipped with a high-resolution MS to investigate exosomal lipids from human serum.

Methods: Exosomal lipids were profiled using MALDI with Fourier-transform ion cyclotron resonance (FTICR)-MS. Four matrices (i.e., α-cyano-4-hydroxycinnamic acid [CHCA], 2,5-dihydroxybenzoic acid, sinapinic acid, and graphene oxide [GO]) and three sample preparation methods (i.e., dried droplet, thin layer, and two layer) were compared for the number of lipid species detected and the relative abundance of each lipid from human serum and human serum exosomes.

Results: In sum, 172 and 89 lipid species were identified from human serum and human serum exosomes, respectively, using all the methods. The highest number of exosome lipid species, 69, was detected using the CHCA matrix, whereas only 8 exosome lipid species were identified using the GO matrix. Among the identified lipid species, phosphatidylcholine was identified most frequently, probably due to the use of a positive ion mode.

Conclusions: Exosomes and human serum showed comparable lipid profiles as determined using MALDI-FTICR-MS. These findings provide a new perspective on exosomal lipidomics analysis and may serve as a foundation for future lipidomics-based biomarker research using MALDI-FTICR-MS.

1 | INTRODUCTION

The involvement of exosomes in cellular communications has expanded our knowledge of normal physiology and pathology. Their characteristics in the delivery of biological components from their cells of origin to the extracellular environment are helpful for understanding various exosome-associated biological conditions, including tumor progression,[1] immune responses,[2] viral pathogenicity,[3] and pregnancy.[4] With technological advances over

the past several decades, the prospect of using exosomes in disease diagnostics, therapeutics, and drug delivery has attracted a great deal of interest.[5,6]

Exosomes are cell-derived nanoparticles 30–150 nm in diameter produced by a process involving double invagination of the plasma membrane and the formation of multivesicular bodies containing intraluminal vesicles, which are then released as exosomes into the extracellular space.[7] Exosomes comprise a lipid bilayer membrane that encapsulates substances, such as proteins, DNA, RNA, lipids, and

metabolites, which may be representative of their cells of origin.[7] Each of these constituents has potential for use as a disease biomarker, and their detection from exosomes instead of entire body fluids considerably reduces sample complexity.[8,9]

Exosome biomarker changes during therapy can provide prognostic information that can be used to determine the best treatment option for diseases.[10] Proteins are the most often investigated components as biomarkers, given many well-established methods available, such as iTRAQ and label-free proteomic analysis.[10,11] Although lipid-based biomarkers have not been studied as extensively as protein-based biomarkers, lipids have been proposed for use as biomarkers. Lipids are essential structural and functional components of exosomes. Abnormal lipid metabolism may contribute to the onset and progression of a number of diseases, such as atherosclerosis, cancer, and obesity.[12] Lipid profiling can provide critical information for understanding diseases, and lipid biomarkers that reflect the states of diseases have been investigated.[13] Lipid biomarkers have been discovered for early detection of hepatocellular carcinoma in individuals with cirrhosis and ovarian cancer.[14,15]

With the emergence of instruments to facilitate the study of lipids, lipid research has become more accessible. Mass spectrometry (MS) has been applied to lipid characterization, particularly paired with liquid chromatography, as the intricacy of lipid characterization necessitates the use of separation methods.[16] However, their lower complexity is one of the most attractive ideas of analyzing lipids derived from exosomes instead of larger cells or whole body fluids.[9] Therefore, chromatographic methods that require longer analysis times may not be necessary for exosomal lipid analysis.

In this study, exosomal lipids derived from human serum were investigated using MALDI-MS with four different matrices: α-cyano-4-hydroxycinnamic acid (CHCA), 2,5-dihydroxybenzoic acid (DHB), sinapinic acid (SA), and graphene oxide (GO). The first three matrices are currently the most commonly used conventional organic matrices in MALDI-MS analysis, whereas GO was selected to profile spectral features at a lower m/z range where organic matrix-derived peaks may overlap with lipid peaks.[17] As the highly abundant peaks from organic matrices can reduce sensitivity for identification of lipids in this low m/z range,[18] GO has been utilized as a matrix for lipidomics analysis in several studies.[19,20]

MALDI sample preparation methods, such as dried droplet, two-layer, and thin-layer methods, were also considered as variables for comparison.[21] The dried droplet method is currently the most commonly used sample preparation method; however, due to the high heterogeneity of the matrix surface, other methods, such as thin-layer and two-layer methods, have been introduced.[22,23] Fourier-transform ion cyclotron resolution (FTICR)-MS was used for the detection of ionized lipids from MALDI to compensate for the lack of chromatography and to ensure high resolution and accuracy of lipid analysis. We compared the identified lipid species from human serum and human serum exosomes and highlighted the differences in spectra across all matrices and sample preparation procedures.

2 | MATERIALS AND METHODS

2.1 | Materials

Pooled human serum was obtained from Innovation Research (Novi, MI, USA). Phosphate-buffered saline (PBS), CHCA, DHB, SA, graphite, and chloroform were purchased from Sigma-Aldrich (St. Louis, MO, USA). Acetonitrile was obtained from Merck (Darmstadt, Germany). Methanol and trifluoroacetic acid (TFA) were obtained from Samchun (Gyeonggi, South Korea). Phosphoric acid was obtained from OCI (Seoul, South Korea). Water was purified using a water purification system (Power I+ water purification system, Human Corp., Seoul, South Korea). All chemicals and reagents used were of analytical or liquid chromatography grade.

2.2 | Exosome enrichment

Exosomes were enriched from human serum by multiple cycles of centrifugation, as described previously.[24] Briefly, serum (4 ml) was first diluted twofold with PBS; centrifuged at 2000g and 12 000g for 30 and 45 min, respectively, using a high-speed centrifuge (2236R, Labogene, Seoul, South Korea); and filtered through 0.2 μm pore size syringe filters (Hyundai Micro, Seoul, South Korea) to remove bacteria and cell debris. The filtered serum was then centrifuged five times, first at 40 000g for 2 h, with subsequent centrifugation steps at 40 000g for 1 h 15 min. The supernatant was removed between centrifugations, and PBS was added. After the final centrifugation, 100 μl of PBS buffer was added to dissolve the pellet, and the resulting solution was stored at −20°C.

2.3 | Exosome characterization

Prior to lipid extraction, exosome characterization procedures were carried out to validate the presence of exosomes and the efficiency of the enrichment process. The methods used for characterization consisted of 1D gel electrophoresis, Western blotting, dynamic light scattering, and MS, all of which were performed in compliance with the guidelines of the Minimal Information for Studies of Extracellular Vesicles 2018 (MISEV2018).[25]

2.3.1 | Gel electrophoresis

Gels were cast by pouring 10% resolving gel into a gel casting plate followed by 5% stacking gel after solidifying the former gel. All gels were prepared according to Harlow and Lane's recipes.[26] Samples (10 μl) were mixed with nonreducing lane marker sample buffer (Thermo Fisher Scientific, Rockford, IL, USA) and incubated at 60°C for 10 min. After the samples were loaded into the wells, electrophoresis was performed at 80 V for 15 min and then at 150 V for 60 min. The gels were dyed with a silver staining kit (Sigma-Aldrich) in accordance with the manufacturer's instructions.

2.3.2 | Western blotting

The samples (10 μl) were incubated for 30 min at 5°C in RIPA lysis buffer (10 μl) comprised of 300mM NaCl, 2.0% Igepal CA-630, 1.0% sodium deoxycholate monohydrate, 0.2% sodium dodecyl sulfate, 100mM Tris–HCl, and 1mM ethylenediaminetetraacetic acid to break down the exosome membrane. Then, gel electrophoresis was performed to separate the proteins from the lysed exosomes, as described in Section 2.3.1. The proteins were then transferred onto polyvinylidene difluoride membranes (7 × 4.2 cm) (Bio-Rad Laboratories, Hercules, CA, USA) by semi-dry transfer at 80 mA for 30 min. The membranes were incubated in blocking buffer consisting of PBS containing 5% skim milk for 1 h at room temperature followed by overnight incubation at 4°C with primary mouse anti-CD63 antibody (ab59479, Abcam, Cambridge, UK) diluted 500-fold in PBS-T (0.1% Tween 20 in PBS). The anti-CD63-treated membranes were rinsed with PBS-T the next day and then incubated for 1 h at room temperature with secondary goat anti-mouse IgG H&L (ab97040, Abcam) in PBS-T (1:1000 dilution). The treated membranes were washed in PBS-T and visualized using a DAB substrate kit (Thermo Fisher Scientific).

2.3.3 | Dynamic light scattering

The samples were diluted 10-fold in cold PBS and briefly sonicated prior to loading into micro cuvettes. A Zetasizer Nano ZS (Malvern Panalytical, Malvern, UK) was first equilibrated for 60 s before adding the cuvette into the chamber. The instrument settings were as follows: material refractive index (RI), 1.4; dispersant RI, 1.331; viscosity, 1.5798 cP; and temperature, 4°C. The number of acquisitions varied according to the count rate, and measurements were done in triplicate. The data were obtained as size distribution (diameter values in nanometer, d.nm) versus number (percentage).

2.3.4 | MALDI-MS

Proteins from enriched exosomes were prepared for MALDI-MS analysis as follows. Samples (10 μl) were dried using a HyperVAC-MAX vacuum concentrator (Hanil Scientific, Gimpo, South Korea). Then, 70% formic acid solution (5 μl) was added to the dried samples for membrane disruption followed by 5 μl of acetonitrile. The samples were then centrifuged at 15 000g for 10 min. The following layer-by-layer sample preparation method[27] was used to load centrifuged samples onto MALDI plates: 1.2 μl of the sample was first deposited on the plate and dried; then 1.2 μl of CHCA matrix solution (10 mg/ml of CHCA in 50% acetonitrile with 2.5% TFA) was placed on top of the sample layer and dried. An IDSys LT MALDI-TOF-MS (Asta, Suwon, South Korea) equipped with an Nd:YLF laser (349 nm) was used to characterize the proteins of enriched exosomes. MALDI-MS was calibrated externally with cytochrome c [m/z 12 359.34 (+1), m/z 6180.17 (+2)] and myoglobin [m/z 16 951.99 (+1), m/z 8476.50

(+2)]. Spectra were acquired in linear positive ion mode in the m/z range of 2000–20 000.

2.4 | Lipid extraction

Folch's liquid partitioning procedure was carried out to extract lipids from enriched exosomes and human serum.[28] Both exosomes and human serum samples (90 μl each) were reconstituted in a mixture of cold chloroform (60 μl) and methanol (30 μl) (2:1) and vigorously mixed for 20 min at room temperature (Intelli mixer SLRM-2M, Mylab, Gyeonggi, South Korea). No pretreatment was performed for human serum samples prior to reconstitution to ensure that all lipids present were included for later characterization. The samples were then centrifuged at 15 000g for 10 min. Water (90 μl) was added to the sample solution, vortexed, and centrifuged to form a biphasic mixture. The aqueous phase was removed, and the organic phase containing lipid extracts was recovered and stored at −20°C.

2.5 | MALDI-FTICR-MS

Several matrices were prepared, including the CHCA matrix solution that was employed for exosome characterization, DHB (10 mg/ml of DHB in 50% acetonitrile with 1% phosphoric acid), SA (10 mg/ml of SA in 50% acetonitrile with 0.1% TFA), and GO (10 mg/ml of GO in 50% acetonitrile with 1% phosphoric acid). GO was prepared by oxidizing graphite, as described previously.[17] Briefly, graphite (0.5 g), potassium permanganate (3.0 g), sulfuric acid (80 ml), and phosphoric acid (20 ml) were agitated at room temperature for 3 days, giving a dark-purple solution. The solution was mixed with 3 ml of hydrogen peroxide and 100 ml of water to prepare graphite oxide and then washed thrice with 1 M HCl and water to reach a pH of 4–5. The graphite oxide was exfoliated during the washing process, thickening the graphene solution to produce GO.[29]

Lipid extracts and matrices were applied to MALDI plates using various sample preparation methods, including the dried droplet,[30] thin-layer,[31] and two-layer[32] methods. The dried droplet method was carried out by mixing the lipid extract with the matrix in the ratio 1:1. The mixture (1.2 μl) was then applied and dried on the MALDI plates. For the thin-layer method, the matrix (1.2 μl) was first applied and dried on the plates before adding the extract (1.2 μl) to the dry matrix. For the two-layer method, the extract–lipid mixture prepared using the dried droplet method was added after applying and drying the matrix (1.2 μl) on the plates.

FTICR-MS spectra of the lipid extracts were obtained using an ultra-high-resolution 15 T FT-ICR-MS (SolariX, Bruker, Billerica, MA, USA) coupled with an Nd:YAG laser (355 nm) located at the Korea Basic Science Institute (KBSI, Ochang, South Korea). Mass spectra were calibrated externally using a mixture of peptide standards comprised of leucine enkephalin (m/z 556.2766), Ala-Ser-His-Leu-Gly-Leu-Ala-Arg (m/z 824.4737), and angiotensin I (m/z 1296.6848). Spectra were acquired in positive ion mode in the m/z range of 400–1400.

2.6 | Data analysis

Bruker Compass DataAnalysis 4.4 and IsotopePattern 3.0 were used to analyze and process FTICR-MS data. The parameters for mass detection were set to a signal-to-noise threshold of 5 and relative intensity threshold of 0.1%–1%, depending on the peak intensity of each spectrum. The m/z value acquired from the spectrum was used for lipid characterization using the LIPID MAPS online database (https://www.lipidmaps.org/), matching the exosomal lipid molecular ion with a mass error of <1 ppm [mass error = (difference between experimental and theoretical mass)/theoretical mass $\times 10^6$]. Orthogonal projections to latent structures-discriminant analysis (OPLS-DA) was performed using MetaboAnalyst (https://www.metaboanalyst.ca/), a web-based data analysis software.

3 | RESULTS AND DISCUSSION

3.1 | Exosome enrichment and characterization

Exosomes were enriched from human serum using a multiple-cycle centrifugation method that uses lower centrifugation speeds but with a greater number of cycles in comparison to standard ultracentrifugation procedures.[24] Although the greater number of cycles requires a longer enrichment time, using a standard centrifuge is relatively inexpensive, and it is more readily available compared to ultracentrifugation.[24] Several studies have described the use of multiple cycles of centrifugation to isolate exosomes for biomarker discovery and proteomic analysis.[11,27]

Gel electrophoresis was used to determine the number of centrifugation cycles required to enrich exosomes. Figure 1A shows 1D gel images of the third to fifth supernatants collected between centrifugation cycles and the isolated pellet containing the exosomes. The decrease in protein bands from the third to the fifth supernatants indicates a decrease in nonexosomal proteins, primarily albumin and immunoglobulins, initially present in the serum.[33,34] The removal of proteins is crucial to determine the purity of the exosomes, although exosome purity was not the primary concern of this study. As stated in MISEV2018, exosome purity depends on the experimental objectives and the exosome end use.[25] Therefore, although a protein band was visible in the fifth supernatant, as shown in Figure 1A, the amount was acceptable as the exosomes were intended for lipidomics analysis. The isolated pellet sample is shown in the next lane. To confirm the presence of exosomes in the pellet, we performed Western blotting analysis using anti-CD63 antibody, where CD63, an exosome membrane protein, was detected after staining with DAB, as shown in Figure S1 (supporting information).

Dynamic light scattering analysis of the isolated pellet revealed particle sizes in the range of typically described exosomes, as shown in Figure 1B. In comparison to the fluctuating particle size of the supernatants (data not shown), the particle size of the pellet was consistent with an average size of 145.5 ± 47.04 d.nm. Characterizing exosomes by size enables exosomes to be distinguished from other extracellular vesicles, such as microvesicles (up to 1000 nm) and apoptotic bodies (up to 5000 nm).[35,36] The presence of exosomes was further confirmed by detecting platelet factor 4 using MALDI-MS, as the exosome marker was distinctively visible at m/z 7766.5 in Figure 1C. Platelet factor 4 is a protein found in exosomes secreted by reticulocytes (immature red blood cells), which explains its detection in exosomes derived from human serum.[37]
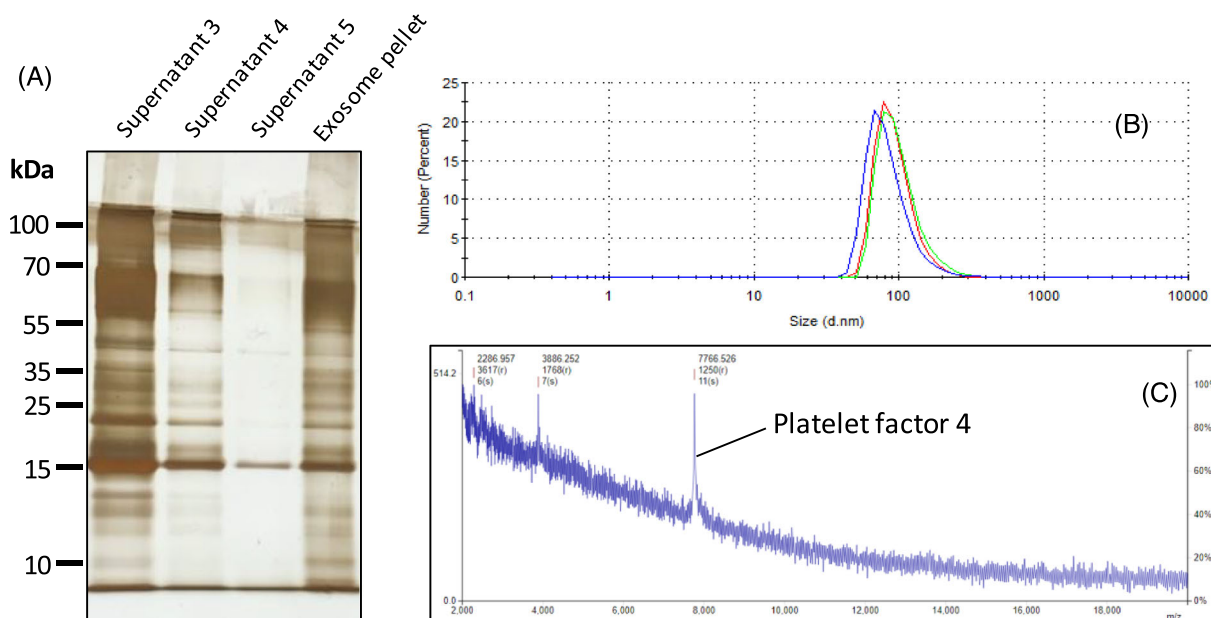
FIGURE 1 Characterization of human serum exosomes. A, 1D gel separation of the third to fifth centrifugation supernatants and the pellet demonstrated the efficacy of exosome enrichment. B, Dynamic light scattering showed particle-size distributions consistent with the size range of exosomes. C, Platelet factor 4, a human serum exosome biomarker, was detected in the MALDI-MS spectrum at m/z 7766. MALDI, matrix-assisted laser desorption/ionization; MS, mass spectrometry [Color figure can be viewed at wileyonlinelibrary.com]

3.2 | Exosomal lipid extraction using the Folch method

There are a number of long-established lipid extraction procedures, although recent methods, such as the Folch,[28] Bligh–Dyer,[38] and methyl-*tert*-butyl ether[39] methods, have been reported to show improvements over earlier procedures. We used the Folch method, which is commonly used to extract lipids from exosomes.[40,41] The Folch method separates lipids in a biphasic mixture of chloroform, methanol, and water. Methanol breaks the hydrogen bonds between lipids and proteins, and the lipids are then partitioned into chloroform.[42] A biphasic system is formed when water is added to the mixture, with the top phase (aqueous) containing nonlipid substances and the bottom phase (organic) containing practically all lipid molecules. It is worth noting that proteins are insoluble in both partitions, resulting in their retention between the two phases. The aqueous phase does not contain proteins because the upper aqueous phase includes approximately 48% methanol.[28] Proteins are unstable and have poor solubility in most polar solvents.[43]

3.3 | MALDI-FTICR-MS analysis of lipidomes

MALDI-FTICR-MS was used to perform lipidomics analysis of human serum and human serum exosomes, with four matrices and three sample preparation methods as variables for comparison. Figure 2 shows the MALDI-FTICR-MS spectra of the lipids from human serum exosomes and human serum, analyzed using the CHCA matrix. The MALDI-FTICR-MS spectra that were analyzed using other matrices, such as DHB, SA, and GO, are shown in Figures S2–S4 (supporting information), respectively. The lipid species identified using MALDI-FTICR-MS are summarized in Table S1 (supporting information). Human serum exosomes and human serum yielded 239 lipid species, featuring 89 lipid species from human serum exosomes and 172 lipid species from human serum, with 22 lipid peaks common to both samples.

The distribution of lipid species by category, that is, sterols (ST), phospholipids (PL), glycerolipids (GL), and sphingolipids (SL) (based on LIPID MAPS nomenclature),[44] is shown in Figure 3A. ST includes cholesteryl ester (CE); PL includes lysophosphatidic acid, lysophosphatidylcholine (LPC), lysophosphatidylethanolamine,
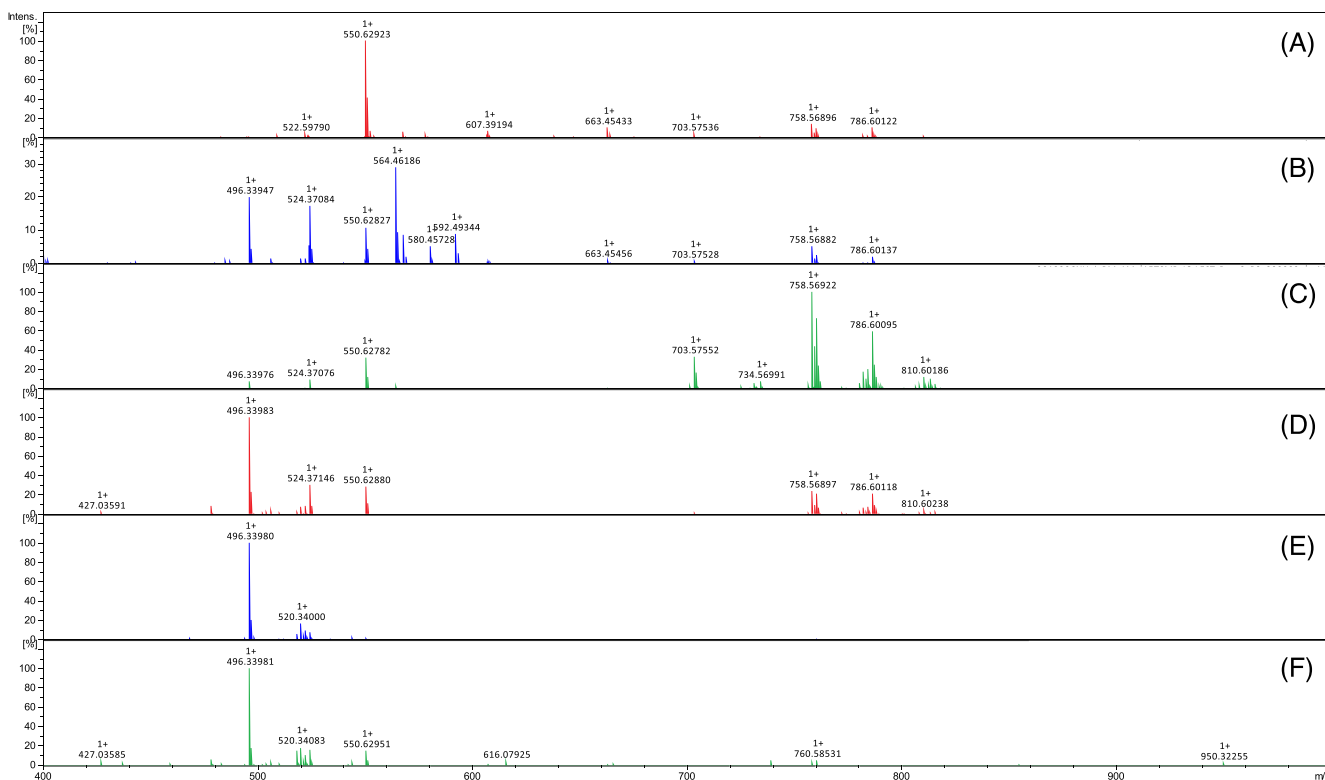
FIGURE 2 MALDI-FTICR-MS spectra obtained using CHCA matrix in the *m/z* 400–1000 range for A, exosome lipids using the thin-layer method; B, exosome lipids using the dried droplet method; C, exosome lipids using the two-layer method; D, human serum lipids using the thin-layer method; E, human serum lipids using the dried droplet method; and F, human serum lipids using the two-layer method. CHCA, α-cyano-4-hydroxycinnamic acid; FTICR, Fourier-transform ion cyclotron resonance; MALDI, matrix-assisted laser desorption/ionization; MS, mass spectrometry [Color figure can be viewed at wileyonlinelibrary.com]
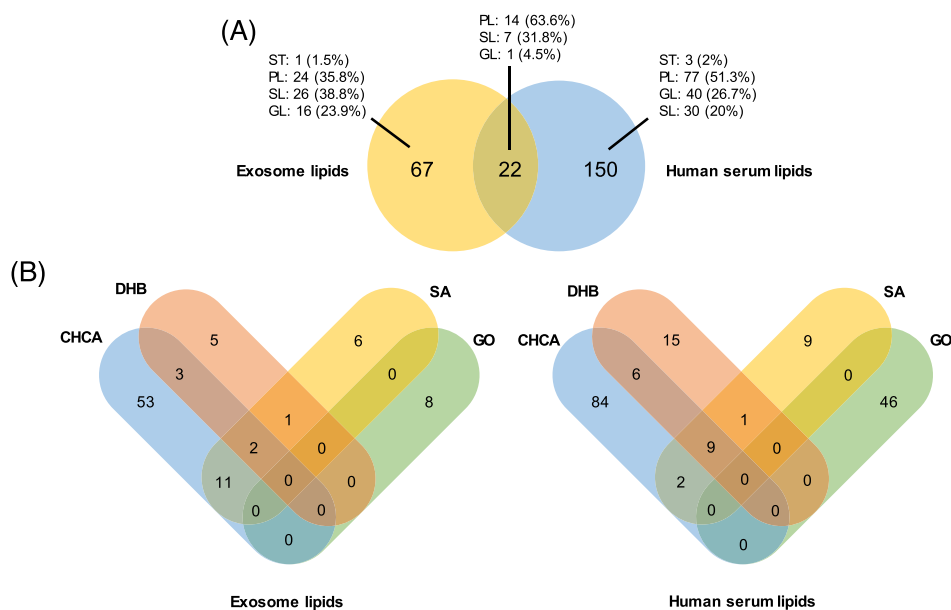
FIGURE 3 Venn diagrams illustrating the distributions of lipids in human serum and exosomes. A, Total lipids identified from human serum and exosomes, regardless of method, and lipid species distribution by category. B, Lipids characterized according to the matrix used, regardless of sample preparation method [Color figure can be viewed at wileyonlinelibrary.com]

lysophosphatidylglycerol, lysophosphatidylinositol, lysophosphatidylserine, phosphatidic acid (PA), phosphatidylcholine (PC), phosphatidylethanolamine (PE), phosphatidylglycerol (PG), phosphatidylinositol (PI), and phosphatidylserine (PS); GL includes diacylglycerol and triacylglycerol (TG); and SL includes ceramide, ganglioside, hexosyl ceramide, sphingomyelin (SM), and sulfatide.

The lipid distributions determined using MALDI-FTICR-MS of both samples confirmed that PL species were more prevalent than GL and SL, with exosome PL species accounting for 44.7% and human serum PL species accounting for 52.9% of the respective total lipid. The data may not reflect the entire lipid composition of exosomes as we did not analyze the lipids in negative ion mode with a relevant matrix, which may detect anionic lipid species, such as *bis*(monoacylglycerol)phosphate, a negatively charged PL species that accumulates during the formation of multivesicular bodies and intraluminal vesicles.[45] No informative results were obtained in MS analysis using the four matrices in negative ion mode because the matrices used were incompatible, possibly due to their acidity.[46] Peterka et al reported that exosomal lipidomics profiling on human plasma using MALDI-MS with 9-aminoacridine (9-AA) in negative mode resulted in the detection of 90% SM, 9.8% PI, and 0.2% sulfatides.[41] In contrast to our findings, their study showed more SL species (SM and sulfatides) than PL species (PI). The results may have corresponded to the ion mode of MS analysis used with relevant matrices. Our results were consistent with other studies that used chromatographic methods, where the SM and PC (including LPC) were shown to be abundant in exosomes following cholesterol.[47]

Figure 3B shows the lipid distribution based on the matrix used. The greatest number of lipids was identified using the CHCA matrix among all four matrices, which was consistent in both exosome and human serum samples. Other organic matrices did not detect many lipids, although some were unique to the respective matrices.

Interestingly, some lipids were commonly identified with the three organic matrices, such as PC 34:2 and PC 36:2 for human serum exosomes and LPC 16:0, LPC 16:1, LPC 18:1, LPC 18:2, LPC 20:4, and PC 36:2 for human serum.

No lipids were identified using both the GO matrix and any of the organic matrices. The observation that the lipids did not overlap implies that the detection of lipids was selectively enhanced toward organic-based and graphite-based matrices, as noted previously.[19] As PC often suppresses the ionization of other PLs in positive ion mode, the GO matrix has been shown to increase the detection of specifically PLs, other than PC.[19] Seven lipid species were identified in our MALDI-FTICR-MS analysis of human serum exosomes using the GO matrix, whereas no PC lipids were observed. In addition, only one PC lipid was included in the 46 lipid species identified by MALDI-FTICR-MS analysis of human serum using the GO matrix.

3.4 | Lipid species dependent on matrix and sample preparation method

Three separate sample preparation methods and four different matrices were used to analyze lipids extracted from exosomes and human serum using MALDI-FTICR-MS. A total of 24 samples were analyzed by MALDI-FTICR-MS precalibrated using peptide standards. Figure 4 shows several lipid species abundant in their respective classes for exosome lipids. On the stacked graphs, the four different matrices are differentiated by brightness, and the three different sample preparation techniques are differentiated by patterns. Table S2 (supporting information) summarizes the distribution of lipid species identified based on the matrix and sample preparation method.

As noted previously, PC and SM species are abundant in exosomes, and we identified 16 PC and 14 SM lipid species, higher than other lipid species in this study. In terms of lipid species
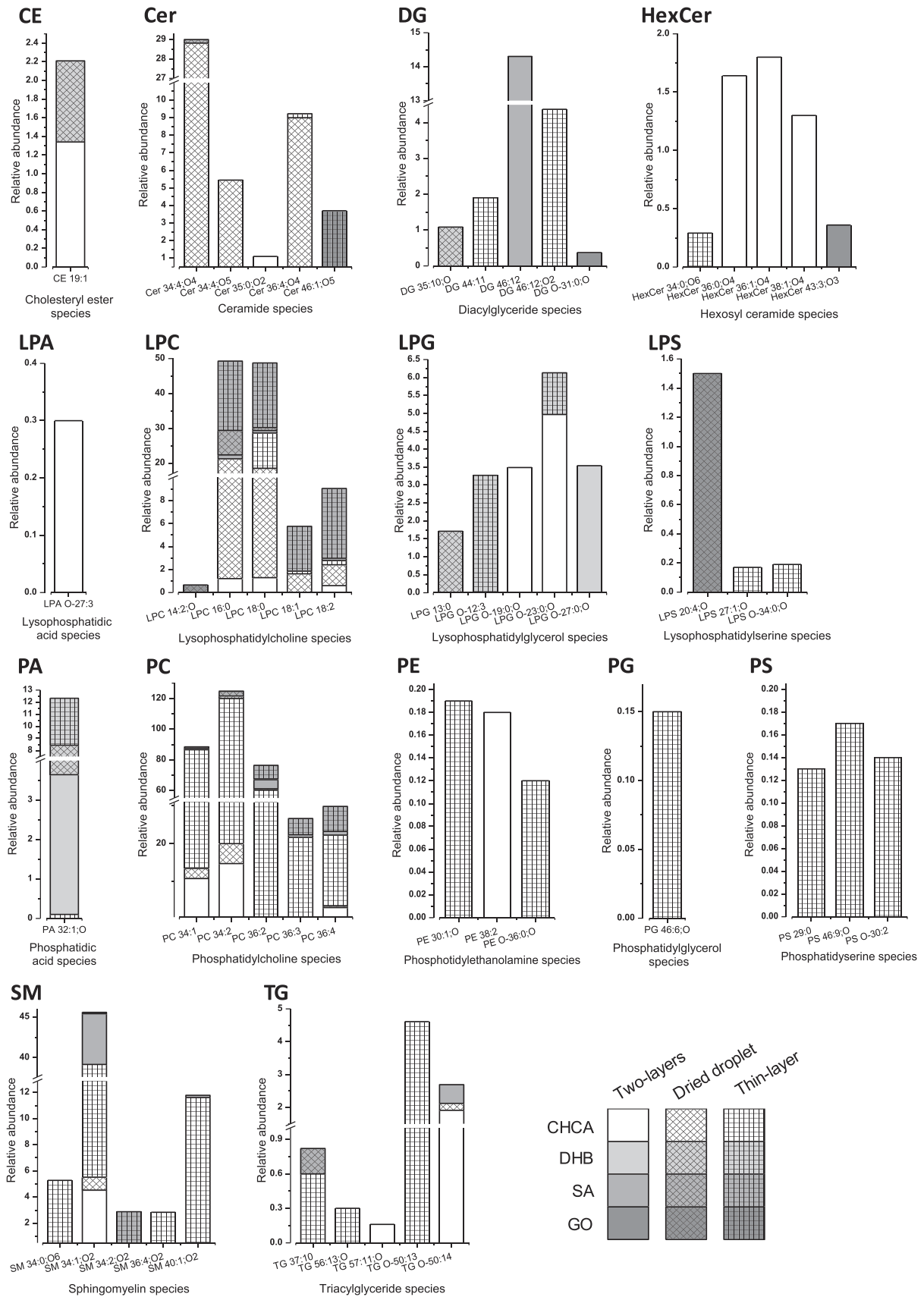
FIGURE 4 Legend on next page.

FIGURE 4 Lipid species distribution of human serum exosomes dependent on the matrix used and the MALDI sample preparation method in terms of relative abundance. The stacked graphs show the most abundant lipid species of the respective classes. Relative abundance represents the intensity of the lipid features in their respective spectrum. MALDI, matrix-assisted laser desorption/ionization

distribution based on the matrix used, almost no PC species were identified using the GO matrix, even in human serum lipid spectra (Figure S5 [supporting information]). In addition, while using the organic matrices, the majority of the lipid signals were identified as $[M + H]^+$, with others detected as various adducts, such as $[M + Na]^+$ and $[M + K]^+$ (Table S1 [supporting information]). However, the GO matrix generated fewer protonated molecules. The lack of PC species and protonated molecules in the GO matrix was most likely due to a strong interaction between the permanent positive charge of the PC head group and the negative charge of GO, as reported previously.[19]

PC and LPC species were prevalent in the CHCA matrix, whereas other PLs, such as PA, PE, PG, and PI, and their lysophospholipid derivatives were suppressed. The DHB matrix, which is more versatile and is widely used,[18,46] could not identify as many lipid species as the CHCA matrix. Several replications, including shot to shot, spot to spot, and sample to sample, were also carried out to ensure that the "sweet spot" phenomena were investigated thoroughly. However, detection using the CHCA matrix was superior to the DHB matrix with regard to the number of lipid species detected. DHB tends to form large, needle-like crystals that are randomly dispersed, resulting in poor uniformity. There have been several attempts to improve its surface uniformity, such as recrystallization by acetonitrile droplet and uniform DHB layer techniques.[48,49] We did not use any uniformity treatment as we intended to perform sample preparation for all matrices similarly, without any additional special improvement for a single matrix. CHCA could generate a more uniform sample–matrix layer, without any uniformity treatment, as compared to other organic matrices.

In terms of sample preparation methods, no consistency in intensity was observed between the same sample preparation methods used on different samples, particularly between thin-layer and two-layer procedures, as shown in Figure 2. The thin-layer approach used on exosome lipids did not work the same as on human serum lipids. For example, the peak at *m/z* 758.569 (PC 34:2) in the exosome lipid for the thin-layer approach (Figure 2A) was intense but not in human serum lipid (Figure 2D), despite the high intensity of the same peak in the two-layer method (Figure 2F). However, both sample preparation methods identified more lipid species compared to the dried droplet method. The lack of detection using the dried droplet method may have been attributable to its low sensitivity, as indicated by its high signal-to-noise ratio. The immiscibility of the solvents used to dissolve the samples and matrices may explain the lack of sensitivity. Even after thorough mixing, the samples may not be present in the portion taken from the sample–matrix mixtures for MALDI sample preparation. This problem may not be encountered in thin-layer and two-layer methods as the samples are placed only on the MALDI plate after the matrix layer dries.

3.5 | Comparison with previously reported human serum exosomal lipids

Whereas this is the first study to use MALDI-FTICR-MS for lipid profiling on human serum exosomes, previous studies have analyzed the lipid contents of human serum exosomes using different MS methods.[50,51] Three of the studies provided in Table 1, including our study, included not only various MS methods but also sample introduction, exosome isolation, and lipid extraction methods. Our study identified the fewest lipid species despite using a high-resolution MS, detecting only 94 in comparison with the other two studies, which identified twice as many lipids. The total number included all lipid species found in our study, regardless of the matrix or sample preparation method used. Chen et al identified the most lipid species, with detection of 458 lipid species using the direct infusion-electrospray ionization (DI-ESI) technique. Both our study and the study of Chen et al used rapid methods to introduce samples into the MS system, but ours was a more selective method considering the matrix used, which resulted in identification of fewer lipids in our study. MS analysis of lipids using the MALDI approach is highly dependent on the matrix used.[18] Selective detection is useful for targeted analysis and is even more effective when used in conjunction with rapid analytical techniques, such as MALDI. DI-ESI is a universal technique that is better suited for untargeted analysis, but it may greatly increase the complexity of the spectrum and, therefore, lipid identification may be challenging and not reproducible.[50]

The incorporation of liquid chromatography into the MS system increases the analysis time but allows for more accurate and comprehensive characterization. Although the total number of lipid species identified by Sun et al was not the highest, the number of lipid species of each lipid category was the highest, as they focused on particular lipid categories, that is, PL and SL. In addition, each species could be further distinguished into more detailed variations, such as oxidized ceramides and deoxyceramides for ceramide species. These variations may be difficult to acquire using the MS approach without a chromatographic method because the relevant peaks may overlap and be suppressed by much stronger peaks.

Exosomes from human plasma may contain the same lipid species as those from human serum because they are derived from the same source, yet the lipid composition may differ due to the higher complexity of plasma. A direct comparison of multiple MS techniques on the lipid content of human plasma exosomes revealed a similar trend to our discussion in which the amount of lipids identified using MALDI-MS was lower than that measured using ultrahigh-performance liquid chromatography-MS and ultrahigh-performance supercritical fluid chromatography-MS.[41] As previously stated, the lipids identified in the MALDI-MS study were correlated with the

TABLE 1 Summary of lipid composition of human serum exosomes analyzed using different MS methods

	Our study	Chen et al[50]	Sun et al[51]	
MS methods	MALDI-FTICR-MS	Direct infusion-TOF-MS/MS	Liquid chromatography-Orbitrap MS	
Samples	Pooled human serum	Human serum from 10 subjects	Pooled human serum and plasma[a]	Human plasma and serum from 12 subjects[a]
Exosome isolation	Multiple cycles of centrifugation	Ultracentrifugation	PureExo isolation kit	PureExo isolation kit
Lipid extraction	Liquid–liquid extraction	Liquid–liquid extraction	Solid-phase extraction	Solid-phase extraction
Lipid category				
CE	1	15	–[b]	–
Cer	12	6	43	46
DG	11	31	–	–
Ganglioside	0[c]	–	8	9
HexCer	8	4	–	–
LPA	1	2	–	–
LPC	8	20	17	13
LPE	0[c]	4	8	7
LPG	6	–	–	–
LPI	0[c]	–	3	0
LPS	3	6	–	–
PA	1	2	–	–
PC	12	69	110	96
PE	3	45	51	40
PG	1	10	–	–
PI	0[c]	–	17	12
PS	3	26	–	–
SM	13	15	49	38
Sulfatide	0[c]	–	5	3
TG	6	203	–	–
Total	89	458	311	264

Abbreviations: CE, cholesteryl ester; DG, diacylglycerol; FTICR, Fourier-transform ion cyclotron resonance; LPA, lysophosphatidic acid; LPC, lysophosphatidylcholine; LPE, lysophosphatidylethanolamine; LPG, lysophosphatidylglycerol; LPI, lysophosphatidylinositol; LPS, lysophosphatidylserine; MALDI, matrix-assisted laser desorption/ionization; PA, phosphatidic acid; PC, phosphatidylcholine; PE, phosphatidylethanolamine; PG, phosphatidylglycerol; PI, phosphatidylinositol; PS, phosphatidylserine; MS, mass spectrometry; SM, sphingomyelin; TG, triacylglycerol.

[a]Exosomes were isolated from a mixture of human serum and plasma.
[b]Dashes (−) indicate lipids that were not detected, could not be confirmed, or did not fall within the range of the analysis.
[c]Lipids with a zero value (0) were not detected in the analysis of exosomes but were detected in the analysis of human serum samples.

matrix and ionization mode used, showing that the method is selective, whereas the LC–MS approach covered a broader range of lipids. In addition, 430 lipid features were identified in an exosomal lipid profiling study of human plasma for distinguishing early- and late-stage non-small-cell lung cancer using nano-ESI Orbitrap fusion tribrid MS (a DI-MS approach), revealing a comparable number of lipids profiled from human serum exosomes using DI-MS.[50,52] The study, however, did not detail the composition of the 430 lipid features as it focused only on 16 lipids selected based on statistical calculations.[52]

3.6 | Multivariate analysis

Multivariate analysis was performed based on the relative abundance and absolute abundance to compare the lipid distributions according to the samples and the preparation method used, as shown in Table S1 (supporting information). The score plot of the supervised OPLS-DA based on the relative abundance and absolute abundance showed two clusters of exosomes and human serum (Figure 5). Several points were found to be distant from the cluster of their respective samples, and these points were from the CHCA matrix of
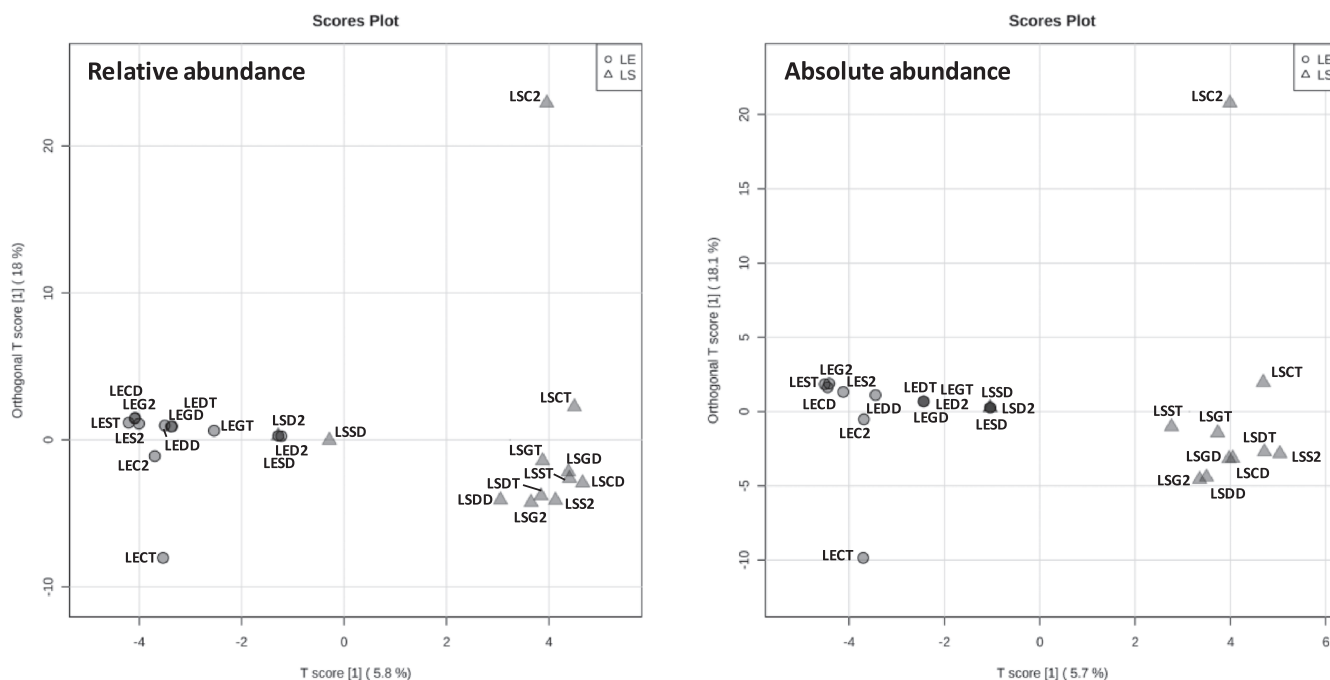
FIGURE 5   Multivariate data analysis of normalized data (normalization by pooled sample from human serum lipids, Pareto scaling) for exosomes (circles) and human serum (triangles) analyzed using MALDI-FTICR-MS. OPLS-DA of A, relative abundance and B, absolute abundance. Abbreviations: LE, exosomal lipids; LS, human serum lipids. The third character indicates the matrix used: C, CHCA; D, DHB; S, SA; G, GO. The fourth character indicates the sample preparation method used: 2, two layer; T, thin layer; D, dried droplet. CHCA, α-cyano-4-hydroxycinnamic acid; DA, discriminant analysis; DHB, 2,5-dihydroxybenzoic acid; FTICR, Fourier-transform ion cyclotron resonance; GO, graphene oxide; MALDI, matrix-assisted laser desorption/ionization; MS, mass spectrometry; OPLS, orthogonal projections to latent structure; SA, sinapinic acid

thin-layer and two-layer methods. In normal statistical analysis, these points were regarded as outliers, as part of the information contained by these points was significantly different from that of the points that clustered together. The most significant feature of these points would be the amount of identified lipid species, which is relevant in this study. Therefore, clustering was seen as less relevant because the matrix and sample preparation method used did not cover most of the lipids in the respective samples.

4 | DISCUSSION

Lipid composition of exosomes has improved our understanding of exosome formation and biological functions, as well as the use of exosomal lipids as disease biomarkers and exosomes as drug carriers. MS methods are unequivocally the most prevalent and effective analytical strategy for lipid studies. Various MS approaches, with or without chromatographic methods, were used to determine the most efficient method for assessing lipids. MALDI-MS has been used for lipidomics analysis due to its rapid and sensitive analysis, although some possible concerns should be addressed.

One limitation, even in the current study, is the lipidome coverage. As discussed in Section 3.5, previous lipidomic profiling using different MS approaches, that is, LC–MS and DI-MS, has

detected more lipids than our study. This finding is due to the lipids' dependence on the matrix used. Several approaches can be considered to improve lipidome coverage, although they were not determined in our work as they were outside the scope of our investigation. One of the attractive alternatives would be surface-assisted laser desorption/ionization (SALDI), as the technique is suitable for detecting small molecules due to the absence of matrix interference. A recent report showed that a polymer-based matrix SALDI-MS analysis of lipids could detect a fair distribution of nonpolar lipids (e.g., TG and CE) that are often suppressed by PL (e.g., PC and PE).[53] Other potential SALDI-MS matrices, such as silicon-based, carbon-based, and nanoparticle-based materials, can be used to enhance lipidome coverage.

Matrices with dual polarities may also be useful for broadening the coverage because different lipids are detected according to ionization modes. 3-Aminophthalhydrazide was shown to be an effective dual-polarity matrix, with PC, PE, and SM being the primary lipids detected in positive mode and PA, PI, and PS in negative mode.[54] The same matrix was also investigated using MS imaging, and spatial resolution improved compared to 9-AA, which increased the sensitivity and lipid coverage in negative ion mode.[54] In addition, a recently introduced MALDI-based technology incorporating laser-induced post-ionization revealed increased lipid coverage due to secondary MALDI-like ionization.[55]

Lipid identification is another challenging aspect of lipidomics due to multiple structures and stereoisomers. In our study, unsaturated lipids were reported based on the number of double bonds present rather than the position of the double bonds, signifying that further research is needed to assess this matter. LC–MS is often preferred for determining lipid isomers, although identifying them in complex biological matrices has still proved difficult, especially when the sample sizes are very small, like exosomes. To facilitate the characterization of lipid isomers, ion activation methods such as ozone-induced dissociation (OzID) and ultraviolet photodissociation (UVPD) have been developed. For OzID, ionized lipids are subjected to ozone vapor in an ion trap MS, allowing the generation of chemically induced fragment ions to determine the double bond position of unsaturated lipids.[56] The UVPD method identifies the location of the double bond while also determining the relative position of the acyl chains on the glycerol backbone by photo-induced cleavage of the carbon–carbon bonds adjacent to the double bond.[57] In addition, ion mobility spectrometry (IMS) has recently been used to study its potential in characterizing lipid isomers, with the IMS being incorporated into LC–MS for multidimensional separation.[58] Although multidimensional measurement provides huge potential for identifying lipid isomers, the raw data are complex and difficult to interpret. Thus, developing software tools, such as the open-source software Skyline, is critical to efficiently process and facilitate confident lipid annotations.[59]

The quantitative aspect of the MALDI-MS approach is frequently regarded as its limitation. The primary reason for this is the occurrence of "sweet spots" that affect reproducibility. Furthermore, suppression by dominating ions can distort the data, as shown in this study, where the PC suppressed other PL species. The preferred strategy for addressing this issue would be to quantify lipids relative to internal standards. However, as previously reported, measuring concentration ratios using the relative intensity of samples and internal standards was highly inaccurate due to the strong influence of the sample analyzed, such as the suppression effect.[60] Using isotope-labeled analyte derivatives such as stable isotope-labeled lipids would be an appropriate internal standard for quantification as it showed better precision and accuracy, although it is underutilized in MALDI-based lipidomics.[60] A study used a deuterated analogue of endogenous PC, that is, PC(16:0 d31/18:1), to successfully quantify endogenous lipids in rat brains.[61] Further enhancing such methods would benefit quantitative lipidomics, particularly in MALDI-MS analysis.

5 | CONCLUSIONS

In summary, we demonstrated the application of MALDI-FTICR-MS to exosomal lipids by comparing several matrices and sample preparation methods. Lipid detection was shown to be dependent on the matrix used, with lipids being highly identified by the CHCA matrix, whereas the GO matrix provided unique lipid detection. The GO matrix found mainly nonprotonated adducts and fewer PC species than the organic matrices. In addition, the use of the positive ion mode increased the likelihood of detecting PL species compared

to the SM species. Although not specific to any PL species, the inclination to identify one of the two major species, such as PL and SM, using one of the ion modes may reduce spectrum complexity, allowing more efficient lipid characterization. Differences in lipid composition between exosomes and human serum were predicted, but the identification of the variation in discovered lipid species, depending on the matrix and sample preparation procedure used, would be beneficial as a reference for future studies.

DATA AVAILABILITY STATEMENT

The data that supports the findings of this study are available in the supplementary materials of this article.

ORCID

Iqbal Jalaludin https://orcid.org/0000-0001-9117-2489

Huu-Quang Nguyen https://orcid.org/0000-0002-8609-3038

Jeongkwon Kim https://orcid.org/0000-0002-0087-1151

REFERENCES

1. Maia J, Caja S, Strano Moraes MC, Couto N, Costa-Silva B. Exosome-based cell-cell communication in the tumor microenvironment. *Front Cell Dev Biol*. 2018;6(18):18. doi:10.3389/fcell.2018.00018
2. Gehrmann U, Näslund TI, Hiltbrunner S, Larssen P, Gabrielsson S. Harnessing the exosome-induced immune response for cancer immunotherapy. *Semin Cancer Biol*. 2014;28:58-67. doi:10.1016/j.semcancer.2014.05.003
3. Rodrigues M, Fan J, Lyon C, Wan M, Hu Y. Role of extracellular vesicles in viral and bacterial infections: Pathogenesis, diagnostics, and therapeutics. *Theranostics*. 2018;8(10):2709-2721. doi:10.7150/thno.20576
4. Mitchell MD, Peiris HN, Kobayashi M, et al. Placental exosomes in normal and complicated pregnancy. *Am J Obstet Gynecol*. 2015;213(4, Supplement):S173-S181.
5. Soares Martins T, Trindade D, Vaz M, et al. Diagnostic and therapeutic potential of exosomes in Alzheimer's disease. *J Neurochem*. 2021;156(2):162-181. doi:10.1111/jnc.15112
6. Herrmann IK, Wood MJA, Fuhrmann G. Extracellular vesicles as a next-generation drug delivery platform. *Nat Nanotechnol*. 2021;16(7):748-759. doi:10.1038/s41565-021-00931-2
7. Kalluri R, LeBleu VS. The biology, function, and biomedical applications of exosomes. *Science*. 2020;367(6478):eaau6977.
8. Jalaludin I, Lubman DM, Kim J. A guide to mass spectrometric analysis of extracellular vesicle proteins for biomarker discovery. *Mass Spectrom Rev*. 2021;e21749. doi:10.1002/mas.21749
9. Mathew M, Zade M, Mezghani N, Patel R, Wang Y, Momen-Heravi F. Extracellular vesicles as biomarkers in cancer immunotherapy. *Cancers (Basel)*. 2020;12(10):2825. doi:10.3390/cancers12102825

10. An M, Lohse I, Tan Z, et al. Quantitative proteomic analysis of serum exosomes from patients with locally advanced pancreatic cancer undergoing Chemoradiotherapy. *J Proteome Res*. 2017;16(4):1763-1772. doi:10.1021/acs.jproteome.7b00024

11. Nguyen H-Q, Lee D, Kim Y, et al. Label-free quantitative proteomic analysis of serum extracellular vesicles differentiating patients of alcoholic and nonalcoholic fatty liver diseases. *J Proteomics*. 2021;245:104278. doi:10.1016/j.jprot.2021.104278

12. Wang W, Zhu N, Yan T, et al. The crosstalk: Exosomes and lipid metabolism. *Cell Commun Signal*. 2020;18(1):119. doi:10.1186/s12964-020-00581-2

13. Wood PL, Cebak JE. Lipidomics biomarker studies: Errors, limitations, and the future. *Biochem Biophys Res Commun*. 2018;504(3):569-575. doi:10.1016/j.bbrc.2018.03.188

14. Sanchez JI, Jiao J, Kwan S-Y, et al. Lipidomic profiles of plasma exosomes identify candidate biomarkers for early detection of hepatocellular carcinoma in patients with cirrhosis. *Cancer Prev Res*. 2021;14(10):955-962. doi:10.1158/1940-6207.CAPR-20-0612

15. Cheng L, Zhang K, Qing Y, et al. Proteomic and lipidomic analysis of exosomes derived from ovarian cancer cells and ovarian surface epithelial cells. *J Ovarian Res*. 2020;13(1):9. doi:10.1186/s13048-020-0609-y

16. Yang JS, Lee JC, Byeon SK, Rha KH, Moon MH. Size dependent Lipidomic analysis of urinary exosomes from patients with prostate cancer by flow field-flow fractionation and Nanoflow liquid chromatography-tandem mass spectrometry. *Anal Chem*. 2017;89(4):2488-2496. doi:10.1021/acs.analchem.6b04634

17. Lee D, Kim Y, Jalaludin I, et al. MALDI-MS analysis of disaccharide isomers using graphene oxide as MALDI matrix. *Food Chem*. 2021;342:128356. doi:10.1016/j.foodchem.2020.128356

18. Leopold J, Popkova Y, Engel KM, Schiller J. Recent developments of useful MALDI matrices for the mass spectrometric characterization of lipids. *Biomolecules*. 2018;8(4):173. doi:10.3390/biom8040173

19. Wang Z, Cai Y, Wang Y, Zhou X, Zhang Y, Lu H. Improved MALDI imaging MS analysis of phospholipids using graphene oxide as new matrix. *Sci Rep*. 2017;7(1):44466. doi:10.1038/srep44466

20. Xu Y, Deng Y, Ye R, et al. MALDI-MS imaging of lipids and small molecules in rat brain tissue based on graphene oxide film pre-coated matrix. *Int J Mass Spectrom*. 2021;464:116573. doi:10.1016/j.ijms.2021.116573

21. Kim J. Sample preparation for matrix-assisted laser desorption/ionization mass spectrometry. *Mass Spectrometry Letters*. 2015;6(2):27-30. doi:10.5478/MSL.2015.6.2.27

22. Patil AA, Chiang CK, Wen CH, Peng WP. Forced dried droplet method for MALDI sample preparation. *Anal Chim Acta*. 2018;1031:128-133. doi:10.1016/j.aca.2018.05.056

23. Yun K, Jalaludin I, Jung SHE, Jang KS, Kim J. Detection of multiply charged protein ions using matrix-assisted laser desorption/ionization mass spectrometry and a force-dried droplet method with a 2-nitrophloroglucinol matrix. *Analyst*. 2022;147(3):505-515. doi:10.1039/D1AN02114A

24. Kim J, Tan Z, Lubman DM. Exosome enrichment of human serum using multiple cycles of centrifugation. *Electrophoresis*. 2015;36(17):2017-2026. doi:10.1002/elps.201500131

25. Théry C, Witwer KW, Aikawa E, et al. Minimal information for studies of extracellular vesicles 2018 (MISEV2018): A position statement of the International Society for Extracellular Vesicles and update of the MISEV2014 guidelines. *J Extracell Vesicles*. 2018;7(1):1535750. doi:10.1080/20013078.2018.1535750

26. Sambrook J, Russell DW. SDS-polyacrylamide gel electrophoresis of proteins. *CSH Protoc*. 2006;2006(4):pdb.prot4540.

27. Nguyen HQ, Lee D, Kim Y, et al. Platelet factor 4 as a novel exosome marker in MALDI-MS analysis of exosomes from human serum. *Anal Chem*. 2019;91(20):13297-13305. doi:10.1021/acs.analchem.9b04198

28. Folch J, Lees M, Sloane Stanley GH. A simple method for the isolation and purification of total lipides from animal tissues. *J Biol Chem*. 1957;226(1):497-509. doi:10.1016/S0021-9258(18)64849-5

29. Huang NM, Lim HN, Chia CH, Yarmo MA, Muhamad MR. Simple room-temperature preparation of high-yield large-area graphene oxide. *Int J Nanomedicine*. 2011;6:3443-3448. doi:10.2147/IJN.S26812

30. Karas M, Hillenkamp F. Laser desorption ionization of proteins with molecular masses exceeding 10,000 daltons. *Anal Chem*. 1988;60(20):2299-2301. doi:10.1021/ac00171a028

31. Xiang F, Beavis RC, Ens W. A method to increase contaminant tolerance in protein matrix-assisted laser desorption/ionization by the fabrication of thin protein-doped polycrystalline films. *Rapid Commun Mass Spectrom*. 1994;8(2):199-204. doi:10.1002/rcm.1290080215

32. Dai Y, Whittal RM, Li L. Two-layer sample preparation: A method for MALDI-MS analysis of complex peptide and protein mixtures. *Anal Chem*. 1999;71(5):1087-1091. doi:10.1021/ac980684h

33. Barrett KE, Boitano S, Barman SM, Brooks HL. Ganong's review of medical physiology twenty. 2010.

34. Leeman M, Choi J, Hansson S, Storm MU, Nilsson L. Proteins and antibodies in serum, plasma, and whole blood-size characterization using asymmetrical flow field-flow fractionation (AF4). *Anal Bioanal Chem*. 2018;410(20):4867-4873. doi:10.1007/s00216-018-1127-2

35. Kakarla R, Hur J, Kim YJ, Kim J, Chwae Y-J. Apoptotic cell-derived exosomes: Messages from dying cells. *Exp Mol Med*. 2020;52(1):1-6. doi:10.1038/s12276-019-0362-8

36. Ståhl A-L, Johansson K, Mossberg M, Kahn R, Karpman D. Exosomes and microvesicles in normal physiology, pathophysiology, and renal diseases. *Pediatr Nephrol*. 2019;34(1):11-30. doi:10.1007/s00467-017-3816-z

37. Carayon K, Chaoui K, Ronzier E, et al. Proteolipidic composition of exosomes changes during reticulocyte maturation. *J Biol Chem*. 2011;286(39):34426-34439. doi:10.1074/jbc.M111.257444

38. Bligh EG, Dyer WJ. A rapid method of total lipid extraction and purification. *Can J Biochem Physiol*. 1959;37(8):911-917. doi:10.1139/y59-099

39. Matyash V, Liebisch G, Kurzchalia TV, Shevchenko A, Schwudke D. Lipid extraction by methyl-tert-butyl ether for high-throughput lipidomics. *J Lipid Res*. 2008;49(5):1137-1146. doi:10.1194/jlr.D700041-JLR200

40. Brzozowski JS, Jankowski H, Bond DR, et al. Lipidomic profiling of extracellular vesicles derived from prostate and prostate cancer cell lines. *Lipids Health Dis*. 2018;17(1):211. doi:10.1186/s12944-018-0854-x

41. Peterka O, Jirásko R, Chocholoušková M, et al. Lipidomic characterization of exosomes isolated from human plasma using various mass spectrometry techniques. *Biochim Biophys Acta Mol Cell Biol Lipids*. 2020;1865(5):158634. doi:10.1016/j.bbalip.2020.158634

42. Wong MWK, Braidy N, Pickford R, Sachdev PS, Poljak A. Comparison of single phase and biphasic extraction protocols for Lipidomic studies using human plasma. *Front Neurol*. 2019;10(879):879. doi:10.3389/fneur.2019.00879

43. Pace CN, Treviño S, Prabhakaran E, Scholtz JM. Protein structure, stability and solubility in water and other solvents. *Philos Trans R Soc Lond B Biol Sci*. 2004;359(1448):1225-1235. doi:10.1098/rstb.2004.1500

44. Liebisch G, Fahy E, Aoki J, et al. Update on LIPID MAPS classification, nomenclature, and shorthand notation for MS-derived lipid structures. *J Lipid Res*. 2020;61(12):1539-1555. doi:10.1194/jlr.S120001025

45. Rabia M, Leuzy V, Soulage C, et al. Bis(monoacylglycero)phosphate, a new lipid signature of endosome-derived extracellular vesicles. *Biochimie*. 2020;178:26-38. doi:10.1016/j.biochi.2020.07.005

46. Schiller J, Süss R, Fuchs B, et al. The suitability of different DHB isomers as matrices for the MALDI-TOF MS analysis of phospholipids: Which isomer for what purpose? *Eur Biophys J*. 2007; 36(4–5):517-527. doi:10.1007/s00249-006-0090-6

47. Skotland T, Sagini K, Sandvig K, Llorente A. An emerging focus on lipids in extracellular vesicles. *Adv Drug Deliv Rev*. 2020;159:308-321. doi:10.1016/j.addr.2020.03.002

48. Nguyen H-Q, Lee D, Kim Y, Kim MS, Jang K-S, Kim J. Recrystallization of dried droplets using acetonitrile to improve surface homogeneity in matrix-assisted laser desorption/ionization mass spectrometric analysis with 2,5-dihydroxybenzoic acid matrix. *Rapid Commun Mass Spectrom*. 2019;33(18):1481-1484. doi:10.1002/rcm.8491

49. Wei Y, Zhang Y, Lin Y, et al. A uniform 2,5-dihydroxybenzoic acid layer as a matrix for MALDI-FTICR MS-based lipidomics. *Analyst*. 2015;140(4):1298-1305. doi:10.1039/C4AN01964D

50. Chen S, Datta-Chaudhuri A, Deme P, et al. Lipidomic characterization of extracellular vesicles in human serum. *J Circ Biomark*. 2019;8: 1849454419879848. doi:10.1177/1849454419879848

51. Sun Y, Saito K, Saito Y. Lipid profile characterization and lipoprotein comparison of extracellular vesicles from human plasma and serum. *Metabolites*. 2019;9(11):259. doi:10.3390/metabo9110259

52. Fan TWM, Zhang X, Wang C, et al. Exosomal lipids for classifying early and late stage non-small cell lung cancer. *Anal Chim Acta*. 2018; 1037:256-264. doi:10.1016/j.aca.2018.02.051

53. Yu J, Kang Y, Zhang H, et al. A polymer-based matrix for effective SALDI analysis of lipids. *J am Soc Mass Spectrom*. 2021;32(5):1189-1195. doi:10.1021/jasms.1c00010

54. Li B, Sun R, Gordon A, et al. 3-Aminophthalhydrazide (Luminol) as a matrix for dual-polarity MALDI MS imaging. *Anal Chem*. 2019;91(13): 8221-8228. doi:10.1021/acs.analchem.9b00803

55. McMillen JC, Fincher JA, Klein DR, Spraggins JM, Caprioli RM. Effect of MALDI matrices on lipid analyses of biological tissues using MALDI-2 postionization mass spectrometry. *J Mass Spectrom*. 2020; 55(12):e4663. doi:10.1002/jms.4663

56. Thomas MC, Mitchell TW, Harman DG, Deeley JM, Nealon JR, Blanksby SJ. Ozone-induced dissociation: Elucidation of double Bond position within mass-selected lipid ions. *Anal Chem*. 2008;80(1):303-311. doi:10.1021/ac7017684

57. Williams PE, Klein DR, Greer SM, Brodbelt JS. Pinpointing double Bond and sn-positions in Glycerophospholipids via hybrid 193 nm ultraviolet Photodissociation (UVPD) mass spectrometry. *J am Chem Soc*. 2017;139(44):15681-15690. doi:10.1021/jacs.7b06416

58. Kyle JE, Zhang X, Weitz KK, et al. Uncovering biologically significant lipid isomers with liquid chromatography, ion mobility spectrometry and mass spectrometry. *Analyst*. 2016;141(5):1649-1659. doi:10.1039/C5AN02062J

59. Kirkwood KI, Pratt BS, Shulman N, et al. Utilizing skyline to analyze lipidomics data containing liquid chromatography, ion mobility spectrometry and mass spectrometry dimensions. *Nat Protoc*. 2022; 17(11):2415-2430. doi:10.1038/s41596-022-00714-6

60. Szájli E, Fehér T, Medzihradszky KF. Investigating the quantitative nature of MALDI-TOF MS. *Mol Cell Proteomics*. 2008;7(12):2410-2418. doi:10.1074/mcp.M800108-MCP200

61. Jadoul L, Longuespée R, Noël A, De Pauw E. A spiked tissue-based approach for quantification of phosphatidylcholines in brain section by MALDI mass spectrometry imaging. *Anal Bioanal Chem*. 2015;407(8):2095-2106. doi:10.1007/s00216-014-8232-7

SUPPORTING INFORMATION

Additional supporting information can be found online in the Supporting Information section at the end of this article.